

Prediction of thermal conductivity of polymer-based composites by using support vector regression

WANG GuiLian, CAI CongZhong^{*}, PEI JunFang & ZHU XingJian

Department of Applied Physics, Chongqing University, Chongqing 400044, China

Received December 16, 2010; accepted March 16, 2011; published online March 30, 2011

Support vector regression (SVR) combined with particle swarm optimization (PSO) for its parameter optimization, was proposed to establish a model to predict the thermal conductivity of polymer-based composites under different mass fractions of fillers (mass fraction of polyethylene (PE) and mass fraction of polystyrene (PS)). The prediction performance of SVR was compared with those of other two theoretical models of spherical packing and flake packing. The result demonstrated that the estimated errors by leave-one-out cross validation (LOOCV) test of SVR models, such as mean absolute error (MAE) and mean absolute percentage error (MAPE), all are smaller than those achieved by the two theoretical models via applying identical samples. It is revealed that the generalization ability of SVR model is superior to those of the two theoretical models. This study suggests that SVR can be used as a powerful approach to foresee the thermal property of polymer-based composites under different mass fractions of polyethylene and polystyrene fillers.

polymer matrix composites, thermal conductivity, support vector regression, regression analysis, prediction

PACS: 81.05.Qk, 81.70.Pg, 07.05.Tp

1 Introduction

In the past decades, polymer-based composites have attracted increasing interest due to their outstanding properties (wear resistance, corrosion resistance, high thermal conductivity, low friction coefficient, etc.) based on the modification of polymer by filling other materials with high thermal conductivity or/and high hardness, etc [1–4]. Therefore, polymer-based composites with excellent physical or chemical performances can be applied in many key areas. The thermal conductivity of polymer-based composites is a significant material property for many applications [5–8]. Due to the fact that most polymers exhibit low thermal conductivity, much attention has been paid to exploit high thermal conductivity for their specific applications.

The properties of the polymer-based composite are

closely related with many factors, including the types, contents, geometric shapes, physical/chemical properties of the fillers and the matrix. In order to develop the polymer-based composites with high thermal conductivity, which can be widely utilized in specific fields (aerospace, automobile industry, textile and chemical industry, etc.), a number of experimental attempts have been made. It was found that the thermal conductivity of polymer-based composites can be efficiently improved by introduction of conductive fillers, and can be influenced by the shape and content of the fillers in matrix [9–12]. At the same time, various semi-empirical or empirical models have been developed to qualitatively simulate the thermal conductivity of dual-phase polymer matrix composites [13–22]. There are only few models developed for three-phase cases by Agari et al. [17] and Zeng et al. [23]. Based on the experiment result of Agari et al. [17], Zeng et al. [23] set up two theoretical models (flake packing model and spherical packing model) and applied them to simulate the thermal conductivity of three-phase

^{*}Corresponding author (email: caiczh@gmail.com)

polymer-based composite under different mass fraction of copolymer (SEBS), mass fraction of polyethylene (PE) and mass fraction of polystyrene (PS). The mean absolute percentage errors (MAPE) calculated by the two models were over 8%. To explore an appropriate approach and improve the model's accuracy is still a challenging problem.

In this study, support vector regression (SVR) combined with particle swarm optimization (PSO) for its parameter optimization, and integrating leave-one-out cross validation (LOOCV), is proposed to model and predict the thermal conductivity of three-phase polymer-based composites under different mass fraction of SEBS, PE and PS, and the predictive results of SVR were compared with those of spherical packing model and flake packing model.

2 Method and materials

2.1 Support vector regression theory

Support vector machine (SVM), proposed by Vapnik and co-workers in 1995, is a statistical learning approach based on structure risk minimization principle [24]. In recent years, it has been successfully applied to solve classification and regression problems in numerous fields, and delivers state-of-the-art performance in real word applications [25–32]. When SVM is employed to tackle the problems of function approximation and regression estimation by the introduction of an alternative loss function, it is called as support vector regression.

Suppose (\mathbf{x}, y) represents a sample, where \mathbf{x} stands for the independent variables and y the dependent variable. In SVR, the basic idea is to map the \mathbf{x} into a higher-dimensional feature space F via a nonlinear mapping $\Phi(\mathbf{x})$, and then to do linear regression in this feature space. Therefore, SVR is to find the linear relation eq. (1) based on a given training dataset $(\mathbf{x}_1, y_1), \dots, (\mathbf{x}_m, y_m)$.

$$f(\mathbf{x}) = \mathbf{w} \cdot \Phi(\mathbf{x}) + b, \quad \Phi: \mathbf{R}^N \rightarrow F, \mathbf{w} \in F, \quad (1)$$

where \mathbf{w} is a vector for regression coefficients, b is a bias. They are estimated by minimizing the regularized risk function $R(C)$, namely:

$$\text{minimize } R(C) = \frac{1}{2} \|\mathbf{w}\|^2 + C \sum_{i=1}^m L_\varepsilon(f(\mathbf{x}_i) - y_i), \quad (2)$$

$$L_\varepsilon(f(\mathbf{x}_i) - y_i) = \begin{cases} 0, & \text{if } |f(\mathbf{x}_i) - y_i| \leq \varepsilon, \\ |f(\mathbf{x}_i) - y_i| - \varepsilon, & \text{if } |f(\mathbf{x}_i) - y_i| > \varepsilon. \end{cases} \quad (3)$$

where m is the number of training samples, C is a penalty factor; ε is a prescribed parameter controlling the tolerance to error. $(1/2)\|\mathbf{w}\|^2$ is used as a flatness measurement of function. The second term in eq. (2), is the so-called empirical risk, which is measured by ε -insensitive loss function $L_\varepsilon(f(\mathbf{x}_i) - y_i)$ and indicates that it does not penalize errors

below ε .

In order to control function complexity, the linear regression function should be smooth as soon as possible, and considering those training samples with a prediction error larger than ε , positive slack variables ξ and ξ^* are introduced to deal with the data points unsatisfied to eq. (3). The eqs. (2) and (3) can be transformed into the primal function $R(\mathbf{w}, \xi_i, \xi_i^*)$:

$$R(\mathbf{w}, \xi_i, \xi_i^*) = \frac{1}{2} \|\mathbf{w}\|^2 + C \sum_{i=1}^m (\xi_i + \xi_i^*),$$

$$\text{subject to } \begin{cases} y_i - \mathbf{w} \cdot \mathbf{x}_i - b \leq \varepsilon + \xi_i, \\ \mathbf{w} \cdot \mathbf{x}_i + b - y_i \leq \varepsilon + \xi_i^*, \\ \xi_i, \xi_i^* \geq 0. \end{cases} \quad (4)$$

where the first term increases the smoothness of regression function to improve its generalization ability, the second term reduces errors. The penalty factor C is a positive constant, determining the tradeoff between the training error and the model smoothness. Building the Lagrange equation:

$$L(\mathbf{w}, \xi_i, \xi_i^*) = \frac{1}{2} \|\mathbf{w}\|^2 + C \sum_{i=1}^m (\xi_i + \xi_i^*)$$

$$- \sum_{i=1}^m \alpha_i ((\varepsilon + \xi_i) + y_i + (\mathbf{w} \cdot \Phi(\mathbf{x}_i)) + b)$$

$$- \sum_{i=1}^m \alpha_i^* ((\varepsilon + \xi_i^*) + y_i + (\mathbf{w} \cdot \Phi(\mathbf{x}_i)) - b)$$

$$- \sum_{i=1}^m (\lambda_i \xi_i + \lambda_i^* \xi_i^*), \quad (5)$$

where, α_i and α_i^* are Lagrange multipliers to be solved. Only the nonzero values of Lagrange multipliers are useful in predicting the regression line, and their corresponding samples are known as support vectors (SVs). Minimum of eq. (5) is obtained by making partial differential coefficients for \mathbf{w} , b , ξ_i , ξ_i^* equal to zeros, namely:

$$\frac{\partial L}{\partial \mathbf{w}} = \mathbf{w} - \sum_{i=1}^m (\alpha_i - \alpha_i^*) \cdot \Phi(\mathbf{x}_i) = 0,$$

$$\frac{\partial L}{\partial b} = \sum_{i=1}^m (\alpha_i - \alpha_i^*) = 0,$$

$$\frac{\partial L}{\partial \xi_i} = C - \alpha_i - \lambda_i = 0,$$

$$\frac{\partial L}{\partial \xi_i^*} = C - \alpha_i^* - \lambda_i^* = 0. \quad (6)$$

Substituted (6) into (5), its dual optimization problem is written:

$$Q = -\frac{1}{2} \sum_{i,j=1}^m (\alpha_i - \alpha_i^*)(\alpha_j - \alpha_j^*)(\Phi(\mathbf{x}_i) \cdot \Phi(\mathbf{x}_j))$$

$$- \varepsilon \sum_{i=1}^m (\alpha_i + \alpha_i^*) + \sum_{i=1}^m (\alpha_i - \alpha_i^*) y_i,$$

$$\text{subject to } \begin{cases} \sum_{i=1}^m (\alpha_i - \alpha_i^*) = 0, \\ \alpha_i, \alpha_i^* \in [0, C]. \end{cases} \quad (7)$$

Therefore, the function regression problem on SVM may come down to quadratic programming problem (7). By maximizing Q , the array \mathbf{w} can be written in terms of the Lagrange multipliers and training samples as:

$$\mathbf{w} = \sum_{i=1}^l (\alpha_i - \alpha_i^*) \Phi(\mathbf{x}_i), \quad (8)$$

where, l is the number of SVs. Finally, the linear relation eq. (1) has the following explicit form:

$$f(\mathbf{x}) = \sum_{i=1}^l (\alpha_i - \alpha_i^*) k(\mathbf{x}, \mathbf{x}_i) + b, \quad (9)$$

where $k(\mathbf{x}, \mathbf{x}_i) = \Phi(\mathbf{x}) \cdot \Phi(\mathbf{x}_i)$ is a kernel function. Choosing different kernel function can generate different SVR model. The commonly used kernel functions include linear kernel, radial basis kernel, polynomial kernel, sigmoid kernel, etc. In this work, we adopted radial basis kernel (10):

$$k(\mathbf{x}, \mathbf{x}_i) = \exp(-\gamma \|\mathbf{x} - \mathbf{x}_i\|^2). \quad (10)$$

2.2 Optimization of SVR parameters with particle swarm

Because the generalization ability of SVR rests entirely on ε of the ε -insensitive loss function, the penalty constant C , and the radial basis kernel function parameter γ , etc., therefore, it is a key to find out the optimal parameter subset (ε , C , γ). In this study, we search the optimal subset (ε , C , γ) with particle swarm optimization (PSO) algorithm, which search the best subset (ε , C , γ) by regulating the velocity and location of particles. Each of particle swarm is made up of a parameter vector (ε , C , γ). The i th particle is regarded as a point in the 3D space and represented as $\mathbf{u}_i = (u_{i1}, u_{i2}, u_{i3})$, its velocity is represented as $\mathbf{v}_i = (v_{i1}, v_{i2}, v_{i3})$, the position of each particle with its best-fit value, that is its local best, is remembered and denoted as $\mathbf{p}_{i\text{best}}$, its global best, which is the position with the best-fit value of all particles, is also recorded as \mathbf{g}_{best} . At each iterative process, the velocity and position of each particle is adjusted by tracking its local best value, global best value and its present velocity, their iterative equations are as follows [33]:

$$\mathbf{v}_i(t+1) = \omega \mathbf{v}_i(t) + c_1 \text{rand}() (\mathbf{p}_{i\text{best}} - \mathbf{u}_i(t)) + c_2 \text{rand}() (\mathbf{g}_{\text{best}} - \mathbf{u}_i(t)), \quad (11)$$

$$\mathbf{u}_i(t+1) = \mathbf{u}_i(t) + \mathbf{v}_i(t+1), \quad (12)$$

where, $\mathbf{v}(t)$, $\mathbf{v}(t+1)$, $\mathbf{u}(t)$, $\mathbf{u}(t+1)$ are respectively the speed and position of present moment and the next moment; rand()

is the random number between 0 and 1; Both c_1 and c_2 are learning factors, normally set as 2; ω is a weighting factor to accelerate the convergence rate, whose value should automatically regulate with the iterative time of algorithm extending, defined generally as:

$$\omega = \omega_{\min} + (N_{\max} - N)(\omega_{\max} - \omega_{\min}) / N_{\max}, \quad (13)$$

where, ω_{\max} and ω_{\min} are respectively the biggest and smallest weight factor, commonly set as 0.9 and 0.4. N is the number of current iteration, N_{\max} is total number of iterations. In this study, mean absolute percentage error (MAPE), which directly reflects the performance of SVR, is selected as fitness function:

$$\text{MAPE} = \frac{1}{m} \sum_{i=1}^m \left| \frac{\hat{y}_i - y_i}{y_i} \right|. \quad (14)$$

2.3 Dataset

The dataset used in this study was generated by Zeng et al. [23], which was acquired experimentally by Agari et al. [17] and was tabulated in Table 1. This dataset comprises the thermal conductivity indexes for 16 specimens by blending different mass fraction of SEBS, PE and PS. The detailed experimental procedure can be referred to ref. [17].

2.4 Modeling strategy

Based on the measured data of thermal conductivity of three-phase polymer-based composites, Zeng et al. deduced two formulas to simulate the thermal conductivity by considering the flaky shape and spherical shape of the fillers, respectively [14]. In this work, SVR via LOOCV was

Table 1 Thermal conductivity of the composites under different mass fraction of SEBS, PS and PE [23]

No.	Mass fraction of SEBS ($\times 10^2$ wt %)	Mass fraction of PE ($\times 10^2$ wt %)	Mass fraction of PS ($\times 10^2$ wt %)	k ($\text{W m}^{-1} \text{K}^{-1}$)
1	0.02	0	0.9800	0.1570
2	0.02	0.098	0.8820	0.164
3	0.02	0.294	0.6860	0.1954
4	0.02	0.784	0.1960	0.3070
5	0.048	0	0.9520	0.1510
6	0.048	0.0952	0.8568	0.1610
7	0.048	0.2856	0.3336	0.1840
8	0.048	0.7616	0.1904	0.2760
9	0.091	0	0.9090	0.1610
10	0.091	0.0909	0.8181	0.1641
11	0.091	0.2727	0.6363	0.1725
12	0.091	0.7272	0.1818	0.2780
13	0.167	0	0.8330	0.1641
14	0.167	0.0833	0.7497	0.1710
15	0.167	0.2499	0.5831	0.1850
16	0.167	0.6664	0.1666	0.2500

applied to model and predict the thermal conductivity by using the same dataset from Agari et al. [17]. In the LOOCV, the data set of n samples was divided into two disjoint subsets including a training data set of size $n-1$ and a test data set of size 1. After developing each model based on the training set, the omitted data was predicted.

Considering the relationship among SEBS, PS and PE, the sum of whose weight percent is equal to 100%, one of the three input factors should be excluded during the modeling process so as to attain a reasonable and accurate SVR model. Therefore, the mass fractions of PE and PS are selected as the input factors for SVR modeling while as the thermal conductivity of composite acted as output variable.

2.5 Evaluation of model's generalization performance

Besides MAPE, mean absolute error (MAE) and correlation coefficients (R^2) are used to evaluate the performance of regression models. They are formulated as following, respectively:

$$MAE = \frac{1}{n} \sum_{j=1}^n |\hat{y}_j - y_j|, \quad (15)$$

$$R^2 = \frac{\left(\sum_{j=1}^n (\hat{y}_j - \bar{\hat{y}})(y_j - \bar{y}) \right)^2}{\left(\sum_{j=1}^n (\hat{y}_j - \bar{\hat{y}})^2 \cdot \sum_{j=1}^n (y_j - \bar{y})^2 \right)}, \quad (16)$$

where, n represents the total number of test samples, y_j stands for the experimental value (or target value) and \hat{y}_j denotes the predicted value for the j th test sample, \bar{y} is the mean target value as well as $\bar{\hat{y}}$ is the mean predicted value for all test samples.

3 Results and discussions

Table 2 gives the experimental and estimated k values predicted by the flake packing model, spherical packing model and LOOCV test of SVR, respectively. Table 3 lists indexes MAE, MAPE and R^2 of the prediction performance among the flake packing model, spherical packing model and LOOCV test of SVR. Figure 1 shows the comparison of measured and estimated thermal conductivity by using SVR-LOOCV, spherical packing model and flake packing model, respectively. Figure 2 is a ternary diagram of depicting the thermal conductivity against different mass fractions of SEBS, PE and PS in terms of SVR model.

From Table 2, it can be observed that, except for one sample numbered as #4, all other samples' absolute percentage errors predicted by LOOCV test of SVR are smaller than those of the spherical packing model and flake packing

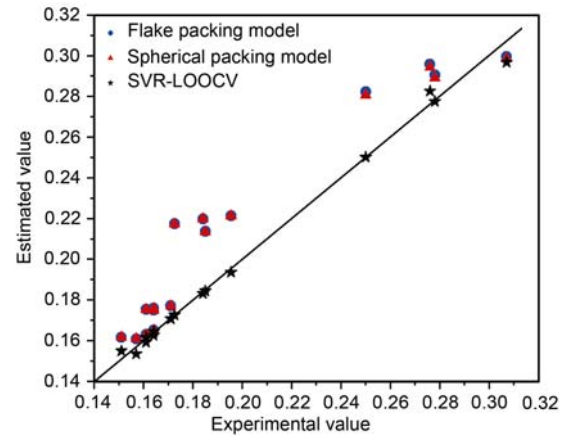


Figure 1 Comparison of experimental values vs. estimated values predicted by flake packing model, spherical packing model and LOOCV test of SVR.

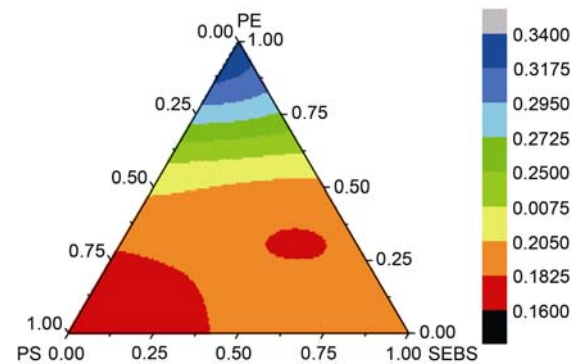


Figure 2 Ternary diagram of predicted thermal conductivity of composite against different mass fraction of SEBS, PE and PS by SVR.

Table 2 Comparison between experimental values and estimated results calculated by the flake packing model, spherical packing model and LOOCV test of SVR.

No.	Exp.	k (W m ⁻¹ K ⁻¹)					
		Flake packing model Cal. [23]	Error (%)	Spherical packing model Cal. [23]	Error (%)	SVR-LOOCV Pred.	Error (%)
1	0.1570	0.1609	2.48	0.1609	2.48	0.1536	-2.17
2	0.1640	0.1751	6.77	0.1749	6.65	0.1627	-0.79
3	0.1954	0.2215	13.36	0.2213	13.25	0.1936	-0.92
4	0.3070	0.2997	-2.38	0.2985	-2.77	0.2968	-3.32
5	0.1510	0.1617	7.09	0.1617	7.09	0.1550	2.65
6	0.1610	0.1755	9.01	0.1753	8.88	0.1616	0.37
7	0.1840	0.2198	19.46	0.2199	19.51	0.1832	-0.43
8	0.2760	0.2958	7.17	0.2945	6.70	0.2827	2.43
9	0.1610	0.1630	1.24	0.1629	1.18	0.1594	-0.99
10	0.1641	0.1761	7.31	0.1759	7.19	0.1646	0.30
11	0.1725	0.2175	26.09	0.2174	26.03	0.1727	0.12
12	0.2780	0.2905	4.50	0.2891	3.99	0.2776	-0.14
13	0.1641	0.1652	0.67	0.1652	0.67	0.1645	0.24
14	0.1710	0.1772	3.63	0.1771	3.57	0.1708	-0.12
15	0.1850	0.2137	15.51	0.2134	15.35	0.1845	-0.27
16	0.2500	0.2823	12.92	0.2807	12.28	0.2502	0.08

model. Meanwhile, the prediction results of two theoretical models are very close to each other, and all except one sample (#4) for the spherical packing model are greater than the related actual values. These results also can be intuitively viewed in Figure 1. Most of points by using LOOCV test of SVR are more close to the straight-line with slope 1 than those of two theoretical models. This reflects that, by comparison with the two theoretical models, SVR model gives the most satisfactory agreement with the experimental values.

It can be viewed from Figure 1 that the right-most point (★) came from the test sample numbered as #4 is more far away from the best-fit line than other two points (●) and (▲), its target value ($0.3070 \text{ W m}^{-1} \text{ K}^{-1}$) is the biggest one among all 16 samples and thus goes beyond the scope of all the 15 training samples. An absolute percentage error (3.32%) forecasted by SVR for this sample is slightly greater than that of either flake packing model (2.38%) or spherical packing model (2.77%). This case revealed that the SVR has a limited extrapolation capacity than those of the theoretical models.

Table 3 is the comparison of the prediction performance among SVR model, spherical packing model and flake packing model. It can be seen from Table 3 that simulated accuracy conducted by the spherical packing model is slightly greater than that of the flake packing model. It can be further found from Table 3 that the MAE ($0.0034 \text{ W m}^{-1} \text{ K}^{-1}$) and MAPE (0.96%) generated by LOOCV test of SVR are both the smallest, and quite smaller than those of the flake packing model (MAE= $0.0168 \text{ W m}^{-1} \text{ K}^{-1}$, MAPE=8.72%) and spherical packing model (MAE= $0.0165 \text{ W m}^{-1} \text{ K}^{-1}$, MAPE=8.60%). At the same time, the correlation coefficients (0.9954) of SVR-LOOCV is much greater than those of the flake packing model (0.9253) and spherical packing model (0.9241).

Figure 2 is a ternary diagram illustrated the calculated thermal conductivity by SVR model against different mass fractions of SEBS, PE and PS, it reflects the synergistic effect of polymer matrix composites on thermal conductivity. One can deduced from Table 1 or Figure 2 that the thermal conductivity of the polymer composite is not simply equal to the weighted sum of the thermal conductivities of pure components of SEBS ($0.191 \text{ W m}^{-1} \text{ K}^{-1}$), PE ($0.3386 \text{ W m}^{-1} \text{ K}^{-1}$) and PS ($0.1603 \text{ W m}^{-1} \text{ K}^{-1}$) [23], otherwise, it will bring about MAPE=8.37%, which is much greater than that (0.96%) of SVR.

Table 3 Comparison of the prediction performance among the flake packing model, spherical packing model and LOOCV test of SVR

Method	MAE ($\text{W m}^{-1} \text{ K}^{-1}$)	MAPE (%)	R^2
Flake packing model [23]	0.0168	8.72	0.9253
Spherical packing model [23]	0.0165	8.60	0.9241
SVR-LOOCV	0.0034	0.96	0.9954

It can be found in Figure 2 that the thermal conductivity is small with low mass fraction of PE (0%–25%), SEBS (0%–40%) and high mass fraction of PS (70%–100%). As the content of PE increasing from 37.5% to 100%, the index of thermal conductivity gradually grows up to the maximum, which is approximately equal to the thermal conductivity of pure PE ($0.3386 \text{ W m}^{-1} \text{ K}^{-1}$). In addition, when the mass fraction of PE exceeds about 50%, the thermal conductivity of the polymer matrix composite would be greater than that of any other pure component (either PS or SEBS). This reveals that addition of polymer PE with higher thermal conductivity can efficiently increase the thermal conductivity of the polymer matrix composite.

As depicted in Figure 2, the nonlinear varying tendency of thermal conductivity of the polymer-based composite blending under different mass fraction would be helpful for the development of polymer matrix composite possessing ideal amount of thermal conductivity.

4 Conclusions

In this study, the model for thermal conductivity under different mass fractions of SEBS, PE and PS, was set up by support vector regression approach combined with particle swarm optimization for its parameter optimization, and the predictive results were compared with those of the flake packing model and spherical packing model. It is illustrated that the mean absolute error and the mean absolute percentage error based on the LOOCV test of SVR models are both the smallest. Based on the SVR model, the ternary diagram based on the predicted thermal conductivity of composite against different mass fraction of SEBS, PE and PS, intuitively describes the relationship between the thermal conductivity of polymer composite and the proportion of pure component, which is consistent with the former experimental result. These indicate that SVR has a theoretical significance and potential practical value in foreseeing the thermal conductivity in development of polymer-based composites.

This work was supported by the Program for New Century Excellent Talents in University of China (Grant No. NCET-07-0903), the Scientific Research Foundation for the Returned Overseas Chinese Scholars of Ministry of Education, China (Grant No. 2008101-1), the Fundamental Research Funds for the Central Universities (Grant Nos. CDJXS10101107, CDJXS10100037), the Natural Science Foundation of Chongqing, China (Grant No. CSTC2006BB5240), and the Innovative Talent Training Project of the Third Stage of "211 Project", Chongqing University (Grant No. S-09109).

- Misri S, Leman Z, Sapuan S M, et al. Mechanical properties and fabrication of small boat using woven glass/sugar palm fibres reinforced unsaturated polyester hybrid composite. *IOP Conf Ser Mater Sci Eng*, 2010, 11: 012015–012027
- Lu P J, Wang Y L, Sun Z G, et al. Polymer-based composites with

- high dielectric constant and low dielectric loss. *Prog Chem*, 2010, 22: 1619–1625
- 3 Gloria A, De Santis R, Ambrosio L. Polymer-based composite scaffolds for tissue engineering. *J Appl Biomater Biomech*, 2010, 8: 57–67
 - 4 Babrekar H A, Kulkarni N V, Jog J P, et al. Influence of filler size and morphology in controlling the thermal emissivity of aluminium/polymer composites for space applications. *Mater Sci Eng B*, 2010, 168: 40–44
 - 5 Lee E S, Lee S M, Shaneffeld D J, et al. Enhanced thermal conductivity of polymer matrix composite via high solids loading of aluminum nitride in epoxy resin. *J Am Ceram Soc*, 2008, 91: 1169–1174
 - 6 Abbasi F, Shojaei A, Katbab A A. Thermal interaction between polymer-based composite friction materials and counterfaces. *J Appl Polym Sci*, 2001, 81: 364–369
 - 7 Lee G W, Park M, Kim J, et al. Enhanced thermal conductivity of polymer composites filled with hybrid filler. *Compos Part A-Appl Sci Manuf*, 2006, 37: 727–734
 - 8 Cheng W L, Zhang R M, Xie K, et al. Heat conduction enhanced shape-stabilized paraffin/HDPE composite PCMs by graphite addition: Preparation and thermal properties. *Sol Energy Mater Sol Cells*, 2010, 94: 1636–1642
 - 9 Sanada K, Tada Y, Shindo Y. Thermal conductivity of polymer composites with close-packed structure of nano and micro fillers. *Compos Part A-Appl Sci Manuf*, 2009, 40: 724–730
 - 10 Alexandre M, Dubois P. Polymer-layered silicate nanocomposites: preparation, properties and uses of a new class of materials. *Mater Sci Eng Rep*, 2000, 28: 1–63
 - 11 Li T L, Hsu S L C. Enhanced thermal conductivity of polyimide films via a hybrid of micro- and nano-sized boron nitride. *J Phys Chem B*, 2010, 114: 6825–6829
 - 12 Lee B, Dai G. Influence of interfacial modification on the thermal conductivity of polymer composites. *J Mater Sci*, 2009, 44: 4848–4855
 - 13 Yue C, Zhang Y, Hu Z L, et al. Modeling of the effective thermal conductivity of composite materials with FEM based on resistor networks approach. *Microsyst Technol Micro Nanosyst Inf Storage Process Syst*, 2010, 16: 633–639
 - 14 Liu J, Yang R G. Tuning the thermal conductivity of polymers with mechanical strains. *Phys Rev B*, 2010, 81: 174122
 - 15 Lin W, Zhang R W, Wong C P. Modeling of thermal conductivity of graphite nanosheet composites. *J Electron Mater*, 2010, 39: 268–272
 - 16 Park Y K, Kim J G, Lee J K. Prediction of thermal conductivity of composites with spherical microballoons. *Mater Trans*, 2008, 49: 2781–2785
 - 17 Agari Y, Ueda A, Nagai S. Thermal conductivity of polyethylene/polystyrene blends containing SEBS block copolymer. *J Appl Polym Sci*, 1992, 45: 1957–1965
 - 18 He H, Fu R L, Han Y H, et al. Thermal conductivity of ceramic particle filled polymer composites and theoretical predictions. *J Mater Sci*, 2007, 42: 6749–6754
 - 19 Nielsen L E. The thermal and electrical conductivity of two-phase systems. *Ind Eng Chem Fundam*, 1974, 13: 17–20
 - 20 Ganapathy D, Singh K, Phelan P E. An effective unit cell approach to compute the thermal conductivity of composites with cylindrical particles. *J Heat Transfer*, 2005, 127: 553–559
 - 21 Nagai Y, Lai G C. Thermal conductivity of epoxy resin filled with particulate aluminum nitride powder. *J Ceram Soc Jpn*, 1997, 105: 197–200
 - 22 Dong Q W, Liu L L, Liu M S. Advancement of the prediction methods of effective thermal conductivity of polymer-based composites (in Chinese). *J Mater Eng*, 2009, (3): 78–81
 - 23 Zeng Q F, Li J Y, Peng X D. Prediction model of thermal properties of polymer-based composites (in Chinese). *Lubr Eng*, 2006, 4: 70–75
 - 24 Vapnik V. The natural of statistical learning theory. New York: Springer, 1995
 - 25 Wen Y F, Cai C Z, Liu X H, et al. Corrosion rate prediction of 3C steel under different seawater environment by using support vector regression. *Corros Sci*, 2009, 51: 349–355
 - 26 Cai C Z, Zhu X J, Wen Y F, et al. Predicting the superconducting transition temperature T_c of BiPbSrCaCuOF superconductors by using support vector regression. *J Supercond Nov Magn*, 2010, 23: 737–740
 - 27 Cai C Z, Wen Y F, Pei J F, et al. Support vector regression prediction of porosity of porous NiTi alloy by self-propagation high-temperature synthesis. *Rare Met Mater Eng*, 2010, 39: 1719–1722
 - 28 Cai C Z, Wang W L, Sun L Z, et al. Protein function classification via support vector machine approach. *Math Biosci*, 2003, 185: 111–122
 - 29 Cai C Z, Han L Y, Ji Z L, et al. SVM-Prot: Web based support vector machine software for functional classification of a protein from its primary sequence. *Nucleic Acids Res*, 2003, 31: 3692–3697
 - 30 Yang Z, Gu X S, Liang X Y, et al. Genetic algorithm-least squares support vector regression based predicting and optimizing model on carbon fiber composite integrated conductivity. *Mater Design*, 2010, 31: 1042–1049
 - 31 Wang C H, Zhong Z P, Li R, et al. Prediction of jet penetration depth based on least square support vector machine. *Powder Technol*, 2010, 203: 404–411
 - 32 Cai C Z, Wang G L, Wen Y F, et al. Superconducting transition temperature T_c estimation for superconductors of the doped MgB_2 system using topological index via support vector regression. *J Supercond Nov Magn*, 2010, 23: 745–748
 - 33 Kennedy J, Eberhart R. Particle swarm optimization. *Proc IEEE Int Conf Neural Networks*, 1995, 4: 1942–1948